

recd 2/12/91 189
319998
NAG 5-389 1
40P

1
2
3
4
5
6
7
8
9
10
11
12
13
14
15
16
17
18
19
20
21

**A Study of the Surface Energy Balance on Slopes in a
Tallgrass Prairie**

D. Nie

Evapotranspiration Lab, Department of Agronomy

Kansas State University

Manhattan, KS 66502

T. Demetriades-Shah

and

E. T. Kanemasu

Department of Agronomy

University of Georgia

Griffin, GA 30223

(NASA-CR-187698) A STUDY OF THE SURFACE
ENERGY BALANCE ON SLOPES IN A TALLGRASS
PRAIRIE (Kansas State Univ.) 40 p CSCL 04A

N91-16473

Unclass

63/46 0319998

Abstract

Four slopes (north, south, east and west facing) were selected on the Konza Prairie Research Natural Area to study the effect of topography on surface energy balance and other micrometeorological variables. Energy fluxes, air temperature and vapor pressure were measured on the slopes throughout the 1988 growing season. Net radiation was the highest on the south-facing slope and lowest on the north-facing slope, and the difference was more than 150 W m^{-2} (20-30%) at solar noon. For daily averages, the difference was 25 W m^{-2} (15%) early in the season and increased to 60 W m^{-2} (30-50%) in September. The east-facing and west-facing slopes had the same daily average net radiation, but the time of day when maximum net radiation occurred was one hour earlier for the east-facing slope and one hour later for the west-facing slope relative to solar noon. Soil heat fluxes were similar for all the slopes. The absolute values of sensible heat flux (H) was consistently lower on the north facing slope compared with other slopes. Typical difference in the values of H between the north-facing and the south facing-slopes were $15\text{-}30 \text{ W m}^{-2}$. The south-facing slope had the greatest day to day fluctuation in latent heat flux as result of interaction of net radiation, soil moisture and green leaf area. The north-facing slope had higher air temperatures during the day and higher vapor pressures both during the day and at night when the wind was from the south.

Introduction

Satellite remote sensing has great potential for the study of climatologically important land surface properties. The International Satellite Land Surface Climatology Project (ISLSCP) was initiated to evaluate in detail the use of earth-orbiting satellite measurements in estimating surface and near surface biophysical properties (Schmugge and Sellers, 1986). To derive quantitative information of land surface properties from satellite observations, surface data are required for model initialization and validation (Sellers and Hall, 1987). One of the major objectives of the First ISLSCP Field Experiment (FIFE), conducted in 1987-1989, was to monitor the surface fluxes and other biophysical properties at the ground.

The surface energy balance and other meteorological properties, such as air temperature and humidity, are required for modeling the interactions between the land surface and atmosphere. In complex terrain, the surface topography plays a major role in governing the energy fluxes and the physical and biological characteristics of the land surface. Therefore, it is important to understand the quantitative relationships between the surface micrometeorological properties and the surface topography, and to understand how slope and aspect affect the surface energy balance. Recently, there have been studies of the energy balance on sloping surfaces for short periods of time (Segal et al., 1985; Gay, 1986; Wendler et al. 1987;

1 Whiteman et al., 1989).

2
3 In order to better understand the influence of slope and aspect on the surface
4 energy balance components and biophysical properties and their diurnal and seasonal
5 variations, it is essential to evaluate and compare the surface fluxes and other surface
6 properties at sites with different slopes and aspects over a time period of a growing
7 season or longer. This study assesses the energy balances on inclined surfaces with
8 different aspects over a time period of a complete growing season. The main goal
9 was to study the effect of topography on surface energy balance and other
10 meteorological and biological variables and their diurnal and seasonal variations.

11 12 13 **Materials and Methods**

14
15 This study was conducted in the Konza Prairie Research Natural Area
16 (KPRNA) south of Manhattan, Kansas, during 1988 as part of FIFE-88. KPRNA,
17 a naturally reserved tallgrass prairie operated by Division of Biology, Kansas State
18 University, constitutes the northwest portion of the 15 km by 15 km FIFE study area
19 (Sellers and Hall, 1987). Four sloping surfaces were selected as experimental sites
20 to measure surface fluxes (Table 1): a 16 degree south facing slope (site 806(2133-
21 BRK)), a 14 degree west facing slope (site 810(3317-BRK)), a 22 degree north facing
22 slope (site 812(1935-BRK)), and a 14 degree east facing slope (site 814(3409-BRK)).

1 The elevations of the sites were similar. The surface soil texture (0-10 cm) for the
2 four sites varied from clay loam to silt loam with soil depth of 12 cm (site 806(2133-
3 BRK)) to 18.5 (site 812(1935-BRK)). The dominant species of vegetation for the
4 sites are prairie grasses: big bluestem (*Andropogon gerardii*) and Indiangrass
5 (*Sorghastrum nutans*). None of the four sites had been burned in the last 4 years. As
6 result, a considerable amount of dead vegetation was left from previous seasons.
7

8 The Bowen Ratio Energy Balance (BREB) technique was used to assess the
9 surface energy balance. BREB is a routine field methodology and is considered one
10 of the most desirable meteorological methods for determining the energy fluxes from
11 rolling and sloping landscapes (Fritschen and Qian, 1989). An experiment was
12 conducted to study the suitability of using a BREB technique on slopes of grassland.
13 The results indicated that the technique gave reasonable estimation of energy fluxes
14 for slopes at the FIFE sites (Nie et al., 1991).
15

16 The Bowen ratio energy balance technique requires data of net radiation, surface
17 soil heat flux, and the Bowen ratio (β), which is the ratio of sensible heat flux to
18 latent heat flux. The Bowen ratio (β) was computed from vertical temperature and
19 vapor pressure gradients; thus measurements of temperature and vapor pressure at
20 two different heights are required.
21

22 At each site, surface soil heat flux was measured with three flux plates installed

1 at a depth of 5 cm from the surface and parallel to the surface. Three
2 copper-constantan thermocouples placed above each plate at depths of 1 cm, 2.5 cm
3 and 4 cm were used to obtain the average soil temperature above the plate, and, this
4 average temperature was used for the calculation of the heat storage in the soil layer
5 above the plate (0-5 cm). The surface soil heat flux was the algebraic sum of the
6 heat stored above the plates and the heat flux through the plates.

7
8 Net radiation was measured with a double dome net radiometer (Radiation
9 Energy Balance Systems, Seattle, WA, model REBS Q*4). Total incoming solar
10 radiation was measured with a silicon cell pyranometer (LI-COR, Lincoln, NE), and
11 diffuse solar radiation was measured with a shadow-band (LI-COR, model 2401s)
12 with a silicon cell pyranometer. All the radiation instruments were installed
13 horizontally. Two corrections were applied to the double dome radiometer
14 measurements to estimate the net radiation as received by the sloping surface:

15
16 (i) After the study, the manufacturer suggested that the double-dome net radiometer
17 gave an overestimate of R_n during the day and an underestimate at night. The
18 double dome net radiometers were then recalled by REBS for updating into a single
19 dome model (Q*5). REBS suggested that data measured with the double-dome net
20 radiometer be corrected. In order to achieve a reasonable correction, we conducted
21 experiments in 1989 to compare the radiometers. First, we compared the Q*5 with
22 the Suomi-Tanner ventilated net radiometer under various sky conditions. The two

22 types of radiometers (Q*5 and Soumi-Tanner) gave basically the same results, which
 2 suggests that the Q*5 gave good estimates of net radiation. Then we compared the
 3 Q*4 with the Q*5 to obtain the relationship for converting the Q*4 output to the
 4 Q*5 type. The following equations were obtained using linear regression:

5 for daytime (positive) net radiation;

$$6 \quad Rn_{corrected} = -20.15 + 0.9635 Rn_{measured} \quad (1)$$

7 for nighttime (negative) radiation;

$$8 \quad Rn_{corrected} = -12.22 + 0.9523 Rn_{measured} \quad (2)$$

9 All the net radiation data which were collected by using the Q*4 in 1988 were
 10 adjusted with these two equations.

11
 12 (ii). Since the measurements were made horizontally, net radiation received by the
 13 slope was computed using the direct-beam correction method (Nie and Kanemasu,
 14 1989).

$$15 \quad \text{Beam}_h = \text{total incoming} - \text{diffuse} \quad (3)$$

$$17 \quad \text{Beam}_s = \text{beam}_h \cos(\theta_i) / \sin(h_o) \quad (4)$$

$$18 \quad Rn_s = Rn_h - \text{beam}_h + \text{beam}_s \quad (5)$$

19 where the subscript (h) and (s) denote the solar flux received on a horizontal surface
 20 and on a slope, respectively; and h_o is the solar elevation. θ_i is the angle between
 21 the direct solar beam and the normal of the slope and $\cos(\theta_i)$ is expressed as:

$$\cos(\theta_i) = \cos(\alpha) \sin(h_o) + \cos(\alpha) \cos(A-B) \quad (6)$$

1 where α is the angle of the slope to the horizontal; B is the slope azimuth angle;
 2 and A is the solar azimuth angle.

3
 4 A battery powered AZET Bowen ratio system designed by Gay and Greenberg
 5 (1985) was employed to measure the Bowen ratio. This system gives measurements
 6 of dry and wet bulb temperatures at two heights, from which the temperature and
 7 vapor pressure gradients can be obtained. Data were collected by an HP-3241A
 8 acquisition system with an HP-71b micro-computer as the control unit. A
 9 measurement was taken from each sensor every 15 seconds for 5 minutes starting
 10 from the beginning of the hour, and then the two psychrometers exchanged
 11 positions. The system waited for 2.5 min for the temperature sensors to equilibrate
 12 with the ambient air before another 5 min of data recording. The system completed
 13 a recording cycle when the psychrometers had two exchanges and returned to the
 14 starting position (15 min).

15
 16 The energy balance was computed every 15 minutes using the following
 17 relationships:

$$18 \quad \beta = \gamma \Delta T / \Delta e \quad (7)$$

$$19 \quad \lambda E = - (R_n + G) / (1 + \beta) \quad (8)$$

$$20 \quad H = - (R_n + G + \lambda E) \quad (9)$$

21 where :

22 γ is the psychrometric constant (0.66 mb/°C at sea level);

- 1 ΔT is the temperature difference at the two heights, in $^{\circ}\text{C}$;
2 Δe is the vapor pressure difference at the two heights, in mb;
3 R_n is net radiation, in W m^{-2} ;
4 G is soil heat flux, in W m^{-2} ;
5 H is sensible heat flux, in W m^{-2} ; and
6 λE is latent heat flux, in W m^{-2} .

7

8 Energy used in photosynthesis and energy stored in the layer of vegetation were
9 considered to be negligible. It is defined that energy flowing away from the surface
10 is negative (the surface loses energy), and energy flowing towards the surface is
11 positive (the surface gains energy). Half hourly data were obtained by averaging the
12 2 records during the 30 minutes.

13

14 Other measurements which were taken included wind speed and direction
15 (simultaneously with the energy balance measurements), soil water content (at least
16 once a week), plant biomass, and leaf area (twice a month). Equipment maintenance
17 was carried out every two days when the weather permitted. This included dumping
18 data, changing batteries, examining output from each sensor, checking the level of
19 radiation sensor, adjusting shadow band, adding water to the psychrometers, checking
20 air flow rate of the psychrometers, replacing dirty wicks, etc. The systems were turned
21 off to prevent instrument damage when there was a strong possibility of a
22 thunderstorm.

Results and Discussion

The Bowen ratio method can fail to provide realistic energy fluxes under certain environmental conditions. From Equation (8), λE will approach infinity as β approaches -1. Ohmura (1982) suggested to reject the calculated flux when β is close to -1. Both Gay (1986) and Whiteman et al. (1989) rejected the calculated fluxes when $-0.75 > \beta > -1.25$. This criterion was used in this study.

There are other circumstances in which the Bowen ratio method fails. One case is when $0 > \beta > -0.75$, and $(\Delta e)(R_n + G) > 0$. When $\beta (H / \lambda E)$ falls between 0 and -0.75, $|H|$ is greater than $|\lambda E|$. Latent heat flux should be in the direction of decreasing vapor pressure. Thus if $\Delta e < 0$, λE is negative, and if $\Delta e > 0$, λE is positive. When $(R_n + G)$ has the same sign as Δe $\{(\Delta e)(R_n + G) > 0\}$, then the available energy has the same sign as λE . This means the surface is losing energy by both λE and $(R_n + G)$. The energy balance fails because the surface gains energy only by H whose absolute value is smaller than λE . The same contradiction happens when β is smaller than -1.25 and $(R_n + G)$ has a different sign from Δe . In both cases Equation (8) gives a λE value that flows in the direction of increasing gradient. Therefore, the calculated fluxes were also rejected in these cases.

For those rejected data, an alternative method by Gay (1986) was used to calculate the fluxes. We arbitrarily assigned the flux which is to flow in the same

1 direction as the available energy (either H or λE) to zero so that the other flux (λE
2 or H) will balance the energy budget (Equation 9).

3 4 Diurnal variations

5
6 Day 88148 (May 27, 1988) and 88195 (July 13, 1988) were chosen to illustrate
7 typical diurnal trends. Table 2 shows the fluxes, air temperature, vapor pressure, soil
8 water and leaf area index for the two days at each site. Both days were free of clouds
9 with southerly wind. Figs. 1-4 show the diurnal variation of the energy balance
10 components at the four slopes.

11
12 The north-facing slope received considerably lower radiation than the other
13 slopes and the south-facing slope had the highest available energy on average or at
14 the peak (Table 2). The difference in R_n between north-facing and south-facing
15 slopes could be 150 W m^{-2} (20-30%) at solar noon. However, the north-facing slope
16 had roughly 1 hour longer in time to receive positive net radiation than the
17 south-facing surface on the two days (Fig. 1). In the north-facing slope, net radiation
18 changed from negative to positive at the same time as that in the east-facing slope,
19 and shifted from positive to negative the same time as the west-facing slope. There
20 was little difference in the amount of radiation received by the east-facing and
21 west-facing slopes, either on maximum R_n or on daily average basis. However, it did
22 show a difference in the time of maximum radiation reception. The east-facing slope

1 had the maximum radiation about an hour before solar noon, while the west-facing
2 slope received its largest radiation fluxes an hour after solar noon. Therefore, there
3 was about two hour difference in the solar peak time between the east-facing and the
4 west-facing slopes (Fig. 1). The north-facing and south-facing slope received their
5 maximum radiation at solar noon. The time of maximum radiation flux on a slope
6 may not necessarily be the time when the angle between the sun and the slope
7 normal is the smallest (maximum $\cos(\theta_i)$). The time depends on the steepness of the
8 slope. Interestingly, there was only about a 30 minute time difference when R_n went
9 from negative to positive in the morning or from positive to negative in the evening
10 but more than an hour difference in solar peak between the south-facing slope and
11 east-facing or west-facing slope (Fig. 1). Therefore the net radiation diurnal curve was
12 asymmetrical for east-facing and west-facing slopes, compared to the diurnal
13 symmetry about solar noon for north-facing and south-facing slopes. The longwave
14 energy losses were around 50 W m^{-2} at night for all four slopes, and the effect of
15 aspect on nighttime net radiation was insignificant.

16
17 The daily average soil heat fluxes on the 4 slopes were similarly low (Table 2,
18 G_{ave}). The maximum fluxes were also relatively small, with range of $40\text{-}50 \text{ W m}^{-2}$
19 and an average of $8\text{-}13 \text{ W m}^{-2}$ (Fig. 2). This may be due to the fact that all the sites
20 were unburned for several years and there was a large amount of dead grass on the
21 soil surface. The time of maximum G on the east-facing or west-facing slope showed
22 a hour shift from that on south-facing slope (Fig. 2). The north-facing slope did show

1 lower G on days with drier conditions and later in the season. The time of day when
2 heat flow was into the ground (negative G) was about the same for north-facing, east
3 and south-facing slope, but was greatly delayed for the west-facing slope. In the
4 afternoon, the east-facing slope started positive G earlier while the north-facing, west-
5 facing and south-facing slope started positive G about the same time. Thus, the
6 south-facing and the north-facing slope had the longest time for negative soil heat
7 flux. This may due to the fact that the north-facing slope had a longer time of
8 positive net radiation, and south-facing slope had less dead vegetation.

9
10 Site differences in sensible heat and latent heat fluxes were more complicated
11 since H and λE depend on the amount of net radiation, soil moisture, amount of
12 green leaf area, amount of dead vegetation, etc. High soil moisture and large leaf
13 area index (LAI) result in high latent heat flux, and thick dead grass layer reduces
14 evaporation and deters soil heat flow. On day 148, north-facing and west-facing
15 slopes had higher latent heat flux and lower sensible heat flux compared to the south-
16 facing and east-facing slopes (Fig. 3 and Table 2). The south-facing slope had the
17 highest available energy but soil water was limited; thus it had the highest negative
18 sensible heat flux H and relatively low latent heat flux λE . The north-facing slope had
19 sufficient soil water so that most of the available energy, although lower than the
20 other slopes, was dissipated into latent heat flux. East-facing and west-facing slopes
21 received similar radiation (daily total), but the west-facing slope had higher soil water
22 and LAI, so that more energy was used in evapotranspiration, compared to the east-

1 facing slope. In fact, the west-facing slope had the highest λE (Fig. 3 and Table 2).
2 This may be the reason why the west-facing slope had condensation (positive λE) at
3 night (Fig. 3b). On day 195, the south-facing slope had the highest R_n and soil
4 water; therefore it had the highest λE although the LAI was small. Both H and λE
5 were lower on the north-facing slope because of the lower R_n . East-facing and
6 west-slope had similar amount of latent heat flux and sensible heat, which were
7 higher than the north-facing and south-facing slopes. The time of maximum value
8 of H and λE also tended to match that of R_n (Fig. 4). Soil moisture was affected by
9 rainfall and the south-facing slope had received higher rainfall in the previous days.

10
11 Fig. 5 shows the diurnal variation of air temperature at the four slopes for the
12 two days. Surprisingly, the north-facing slope had the highest air temperature for
13 most of the daytime with difference up to 2°C , but was slightly lower at night. The
14 south-facing slope was the coolest on the two days. One reason could be the
15 southerly wind. On the north-facing slope, the wind speed was lowest among the
16 slope thus heat (although the sensible heat exchange was low) was allowed to
17 accumulate in the surface air layer in which measurements were made. Compared to
18 the west-facing slopes, the east-facing slope was warmer in the morning and cooler
19 in the afternoon. This may be due to the higher sensible heat flux when the slope was
20 facing the sun. Wind was not a factor for the difference between east-facing and
21 west-facing slopes when the air flow was from the south. On day 195, the east-facing
22 slope had similarly higher temperatures as the north-facing slope (Fig. 5b). This may

1 be due to the lower soil moisture at site 814(3409-BRK) (21.1%, lowest among the
2 four sites, see Table 2), so more energy was used in heating the air.

3
4 The diurnal variation of vapor pressure on the two days for the four sites is shown
5 in Fig. 6. The south-facing slope had the lowest vapor pressure both during the day
6 and at night. There were large differences in the vapor pressure among the slopes
7 (0.4-0.6 KPa). The north-facing slope had higher humidity because water vapor could
8 build up near the surface with southerly wind. For the east-facing and west-facing
9 slopes, vapor pressure was high on day 148 (Fig. 6a) and relatively low on day 195
10 (Fig. 6b). One reason could be the large differences in soil water content. The soil
11 moisture on both slopes had dropped 7-9% (see Table 2).

12 13 14 Seasonal variations

15
16 Data from day 130 (May 9) to 250 (September 6) were included in the
17 seasonal analysis. As mentioned earlier the systems were shut down during inclement
18 weather, so there were a considerable amount of missing data. Radiometers on
19 east-facing and west-facing sites were removed for another study on deployment of
20 the slope radiation from day 127-134 and day 220-233; thus, there were no flux data
21 from these two sites on these days. Days with more than two hours of missing data
22 during daytime were excluded. For cases with one missing data, which often occurred

1 when a site was serviced, linear interpolation was applied to the recording of the site
2 to fill in the missing data. If two or more recordings were missing, then the missing
3 values were estimated using the linear time interpolation and space interpolation
4 according to values of other sites.

5
6 Daily average fluxes are plotted over the season in Fig. 7 and Fig. 8, and the
7 seasonal variations of air temperature and vapor pressure of the slopes are shown
8 Fig. 9. Discussions are mainly focused on north-facing and south-facing slopes since
9 the east-facing slope and the west facing slope had similar daily average fluxes and
10 the values were generally between those of the north-facing and the south facing
11 slopes.

12
13 On sunny days, the daily average net radiation showed a trend of south-facing
14 slope > east-facing or west-facing slope > north-facing slope. These differences
15 become larger later in the season when the solar elevation was low (Fig 7a). The
16 average daily net radiation on the north-facing slope declined by about 80 W m^{-2} ,
17 from over 180 W m^{-2} around day 200 to about 100 W m^{-2} around day 250 on clear
18 days. The south-facing slope only decreased by about 30 W m^{-2} during this same
19 period. The difference in daily average of Rn across slopes varied from about 15 W
20 m^{-2} (8%) around day 195 to more than 60 W m^{-2} (30-50%) around day 250. In the
21 summer, the north-facing slope had a longer time period for positive net radiation
22 and this tended to compensate for the lower net radiation during most of the

1 daytime. Also beam radiation is not linearly related to the angle between the sun
2 and normal of a slope but varies with the cosine of this angle. Therefore, the
3 radiation received by the slope decreases more rapidly with increase of the angle
4 between the sun and the normal of the slope when the angle is large.

5
6 From Fig. 7b, it can be seen that absolute value of the soil heat flux was
7 generally larger on the south-facing slope, compared to values on the north-facing
8 slope. However, there were a few cases when the south-facing slope had lower soil
9 heat flux than the north-facing slope possibly due to higher soil water content on the
10 south-facing slope. There were fluctuations from day to day, with larger fluctuation
11 in the middle of the season, compared to early and late season. There was a general
12 trend of decreasing soil heat flux over the growing season, which may be related to
13 vegetation cover. At the beginning of the season, the net radiation was relatively
14 high, although not the highest in the season (Fig. 7a), and the green leaf area index
15 was very low; the radiation was mainly partitioned into soil heat and sensible heat
16 fluxes. Therefore, the soil heat flux was the highest at this part of the season. With
17 the rapid increase of green leaf in the early season (day 130-180), the latent heat flux
18 (λE), which is the energy used in evapotranspiration, became dominant, and less
19 radiation reached the soil surface due to shading by the vegetation, thus the soil heat
20 flux decreased although net radiation increased. The daily evapotranspiration varied
21 greatly from day to day depending on available soil moisture which subsequently
22 caused the large fluctuations of G in the mid-season. Late in the season, although λE

1 decreased, soil heat flux kept decreasing because the radiation decreased and the
2 thick grass cover reduced G.

3
4 The north-facing slope had lower H than the south-facing slope throughout the
5 season (Fig. 8a). There are two main reasons: (1) the north-facing slope had lower
6 net radiation; and (2) the soil water content was relatively high most of the time on
7 the north-facing slope. As the result, a relatively larger portion of energy was used
8 in evapotranspiration at the north-facing slope, thus H became small. The seasonal
9 trend shows that the absolute value of H was large early in the season when there
10 was low green leaf area. This value decreased as vegetation cover increased, and
11 increased again late in the season as the plants senescence (Fig. 8a).

12
13 Fig. 8b shows the variation of latent heat flux on the 4 slopes. The seasonal
14 pattern agrees with the typical "green-up - peak greenness - senescence" trend (Seller
15 and Hall, 1987) of a tallgrass prairie as shown by leaf area index (Fig. 9a), although
16 there were fluctuations in λE from day to day due to variation of net radiation and
17 soil moisture. The south-facing slope showed the greatest variation in latent heat flux
18 compared to the other sites. On sunny days with high soil water content, the south-
19 facing slope had the highest λE . However, on days with low λE , the south-facing
20 slope had lower λE than the north-facing slope. This is because the south-facing
21 slope dries more quickly with greater λE , and soil water becomes the limiting factor
22 for λE . The seasonal variation of soil moisture content (see Fig. 9b) shows greater

1 fluctuations at the south-facing slope, compared to the other sites. The south-facing
2 slope also had shallower soil depth (Table 1), therefore less water could be stored in
3 the soil.

4
5 The relationship among latent heat flux, leaf area index and soil moisture can be
6 shown more clearly when latent heat flux is converted to evapotranspiration
7 (mm/day), since λE is the energy used in evapotranspiration (ET). Fig. 10 shows the
8 variation of leaf area and ET at the south-facing slope during the season. The two
9 peaks in LAI (leaf area index) correspond to the two high ET periods while the low
10 LAI corresponds to the low ET. Soil moisture also explains the seasonal variation
11 of ET as illustrated in Fig. 11. The variation in soil moisture was reflected by the
12 changes in ET except during the early part of the season when the LAI was low.
13 Since these sites were unburned, ET was especially sensitive to the green leaf area
14 because the dead vegetation cover limits direct soil evaporation. Net radiation, leaf
15 area and soil water content influence the latent heat flux of a surface. They also
16 affect each other and thus cause differences among slopes. For instance, soil water
17 content and leaf area can affect the surface albedo which in turn influences the net
18 radiation.

19
20 Fig. 12 shows the seasonal variations of air temperature (a) and vapor pressure
21 (b). In most cases, the north-facing slope was slightly warmer than the south-facing
22 slope. As discussed earlier, the southerly wind resulted in higher air temperature on

1 north-facing slope. Southerly wind was the dominate wind direction at KPRNA.
2 Since the vapor pressure was lower on the south-facing slope and higher on the
3 north-facing slope as discussed earlier, the daily average vapor pressure was highest
4 on the north-facing slope and lowest on the south-facing slope throughout the season
5 (Fig. 12b).

7 Summary and Conclusions

8
9 Topography has a significant influence on the surface energy balance and other
10 micrometeorological properties. The major effect is the amount of radiation each
11 surface receives. The time when the surface receives maximum net radiation also
12 varies with the aspect and the inclination of the surface. In addition, there are
13 differences among slopes in duration of positive net radiation because of differences
14 when R_n changes from positive to negative and vice versa. These radiative features
15 will affect the partitioning of the available energy into other energy balance
16 components such as sensible and latent heat fluxes and affects other
17 micrometeorological properties.

18
19 In the four sloping surfaces under this study, the following can be attributed to
20 the effect of topography:

- 21
22 1. The difference in net radiation can be 150 W m^{-2} or 20-30% at solar noon and

1 30 W m^{-2} or 15-20% on daily average basis between north-facing and south-facing
2 slopes, and these radiation differences increase with decreasing solar declination. The
3 difference in daily average net radiation between the north-facing slope and the
4 south-facing slope was about 15 W m^{-2} or 8% and increased later in the season to
5 more than 60 W m^{-2} or 30-50%. For the east-facing or the west-facing slope, there
6 was over one hour shift in the time of radiation peak from solar noon and about half
7 an hour change in sunrise and sunset time. The north-facing slope receive positive
8 radiation for about one hour longer than the south-facing slope. The effect of aspect
9 on nighttime longwave radiation appeared to be non-significant.

10
11 2. The daily soil heat fluxes were relatively low for all four slopes, averaging 8-13
12 W m^{-2} with maximum of 50 W m^{-2} for the two typical days presented. During the
13 time period of data collection, soil heat flux was the highest at the beginning season
14 (early May) and decreased through the season.

15
16 3. The north-facing slope had lower sensible heat flux (H) during the season,
17 compared to the south-facing slope, with few exceptions. The H values depended
18 primarily on net radiation and soil water content. Typical values of differences in
19 sensible heat flux between the south-facing and north-facing slopes ranged from 15-30
20 W m^{-2} .

21
22 4. The south-facing slope had the greatest day to day fluctuation in latent heat flux.

1 On sunny days, it had higher λE when soil water content was high, due to the higher
2 energy source for transpiration, and therefore a greater depletion of soil water.
3 Therefore λE declined faster due to the limitation of soil water compared to the
4 north surface. This can result in water stress and limit plant growth.

5
6 5. The south-facing slope had lower air temperature (up to 2 °C) during the day and
7 slightly higher temperature at night compared to the north-facing slope, when the
8 wind was from the south which is the dominant wind direction in KPRNA during the
9 growing season. The north-facing slope was more humid both day and night with a
10 difference of 0.4-0.6 KPa in vapor pressure. The vapor pressure on the north-facing
11 slope was higher throughout the season, compared to the south-facing slope.

12
13 The soil moisture and vegetation cover also interact with the surface
14 topography to influence the surface energy balance components and other properties.
15 The wind direction is also a critical factor in determining how the surface topography
16 affect the fluxes.

17 18 Acknowledgement

19
20 This study was funded by the National Aeronautics and Space Administration
21 of the United States of America under grant NAG-5-389.

References

- Fritschen, L. J., and P. Qian. 1989. Net radiation, sensible and latent heat flux densities on slopes computed by the energy balance method. In: Proceedings of the 19th Conf. on Agricultural and Forest Meteorology, Charleston, SC. American Meteorological Society, Boston, MA.
- Gay, L. W. 1986. Evaluation of surface radiation and energy balance stations on the Konza Prairie. Report prepared for NASA Grant No. NAG 5-521, School of Renewable Natural Resources, University of Arizona, Tucson, AZ 85721.
- Gay, L. W., and R. J. Greenberg. 1985. The AZET battery-powered Bowen Ratio system. Proc., 17th Conf. Agric. and Forest Meteor. p. 181-182. Amer. Meteor. Soc., Boston.
- Nie, D., and E.T. Kanemasu. 1989. Comparison of net radiation on slopes. In: Proceedings of the 19th Conf. on Agric. and Forest Meteor., Charleston, SC. American Meteorological Society, Boston, MA.
- Nie, D., I. Flitcroft, and E. T. Kanemasu. 1991. An investigation on the Bowen ratio technique on a slope in the FIFE site. Submitted to Agric. and Forest Meteor.
- Ohmura, A. 1982. Objective criteria for rejecting data for Bowen ratio flux calculations. J. Appl. Meteor., 21: 595-598.
- Schmuagge, T., and P. J. Sellers(ed.). 1986. Experiment Plan for FIFE. Report of FIFE Science Working Group. NASA Internal Document, NASA/GSFC, Greenbelt, MD 20711.
- Segal, M., Y. Mahrer, R. A. Pielke, and Y. Ookouchi. 1985. Modeling

transpiration patterns' of vegetation along south and north facing slopes during the subtropical dry season. Agric. For. Meteor. 36: 19-28.

Sellers, P. J., and F. G. Hall(ed.). 1987. Experiment Plan. International Satellite Land Surface Climatology Project. NASA Internal Document, NASA/GSFC, Greenbelt, MD 20711.

Wendler, G., N. Ishikawa, and Y. Kodama. 1987. The heat balance of the ice slope of Adelie land, Eastern Antarctica. J. Appl. Meteor. 27: 52-65.

Whiteman, C. D., K. J. Allwine, L. J. Fritschen, M. M. Orgill, and J. M. Simpson. 1989. Deep valley radiation and surface energy budget microclimate. Part II: Energy budget. J. Appl. Meteor. 28: 427-437.

List of Figures

Fig. 1. Diurnal variation of net radiation as affected by slope: a. day 148 (May 27, 1988), b. day 195 (July 13, 1988).

Fig. 2. Diurnal variation of soil heat flux as affected by slope: a. day 148 (May 27, 1988), b. day 195 (July 13, 1988).

Fig. 3. Diurnal variation of sensible and latent heat fluxes affected by slopes on may 27, 1988: a. sensible, and b. latent.

Fig. 4. Diurnal variation of sensible and latent heat fluxes as affected by slopes on July 13, 1988: a. sensible, and b. latent.

Fig. 5. Diurnal variation of air temperature as affected by slope: a. day 148 (May 27, 1988), and b. day 195 (July 13, 1988).

Fig. 6. Diurnal variation of vapor pressure as affected by slope: a. day 148 (May 27, 1988), and b. day 195 (July 13, 1988).

Fig. 7. Seasonal variation of surface energy fluxes as affected by slope: a. net radiation, and b. soil heat flux.

Fig. 8. Seasonal variation of surface energy fluxes as affected by slope: a. sensible flux, and b. latent flux.

Fig. 9. Seasonal variation of soil moisture and leaf area index

Fig. 10. Seasonal variation of ET as affected by leaf area index on the south-facing slope.

Fig. 11. Seasonal variation of ET as affected by soil moisture on the south-facing slope.

Fig. 12. Seasonal variation of air temperature and vapor pressure as affected by slope: a. air temperature, and b. vapor pressure.

Table 1. Summary of Geographical Characteristics of the Sites

site #	slope (degree)	aspect (degree)	elevation (m)	latitude (° , ' , ")	longitude (° , ' , ")	soil depth	soil texture
806 (2133-BRK)	16	south(180)	429	39 05 37	96 32 39	12.1	clay loam
810 (3317-BRK)	14	west (270)	420	39 04 28	96 35 25	16.0	silt loam
812 (1935-BRK)	22	north(358)	425	39 05 49	96 32 58	18.5	clay loam
814 (3409-BRK)	14	east (90)	420	39 04 15	96 34 39	16.5	loam

Table 2. Data Summary for Two Typical Days: Days 148 and 195

Day of year	Site aspect	R _n _{max} W m ⁻²	R _n _{ave} W m ⁻²	G _{ave} W m ⁻²	H _{ave} W m ⁻²	λE _{ave} W m ⁻²	T _{ave} ° C	e _{ave} KPa	Soil water by weight	Total LAI
148	south	678	189	-10	-59	-120	22.06	1.003	21.3%(146)	0.64(145)
148	west	636	180	-8	-32	-140	22.14	1.42	32.5%(146)	0.65(147)
148	north	539	164	-10	-22	-132	22.69	1.394	36.5%(146)	0.45(145)
148	east	639	185	-10	-55	-120	22.43	1.456	28.4%(146)	0.51(147)
195	south	691	193	-12	1	-182	29.17	2.450	32.5%(195)	0.96(190)
195	west	644	179	-13	-8	-159	29.54	2.895	23.1%(195)	2.04(193)
195	north	540	187	-11	-15	-161	29.64	2.638	27.6%(195)	1.46(190)
195	east	642	187	-11	-15	-161	29.64	2.638	21.1%(195)	1.55(193)

- note: 1. On day 195, data from 0:00-9:00 were missing at west slope
2. averages were for 24 hour period.
3. soil moisture was for the depth of 0-10 cm
4. numbers in parentheses indicate the day of year when the measurement was taken

Fig. 1. Diurnal variation of net radiation as affected by slope: a. day 148 (May 27, 1988), b. day 195 (July 13, 1988).

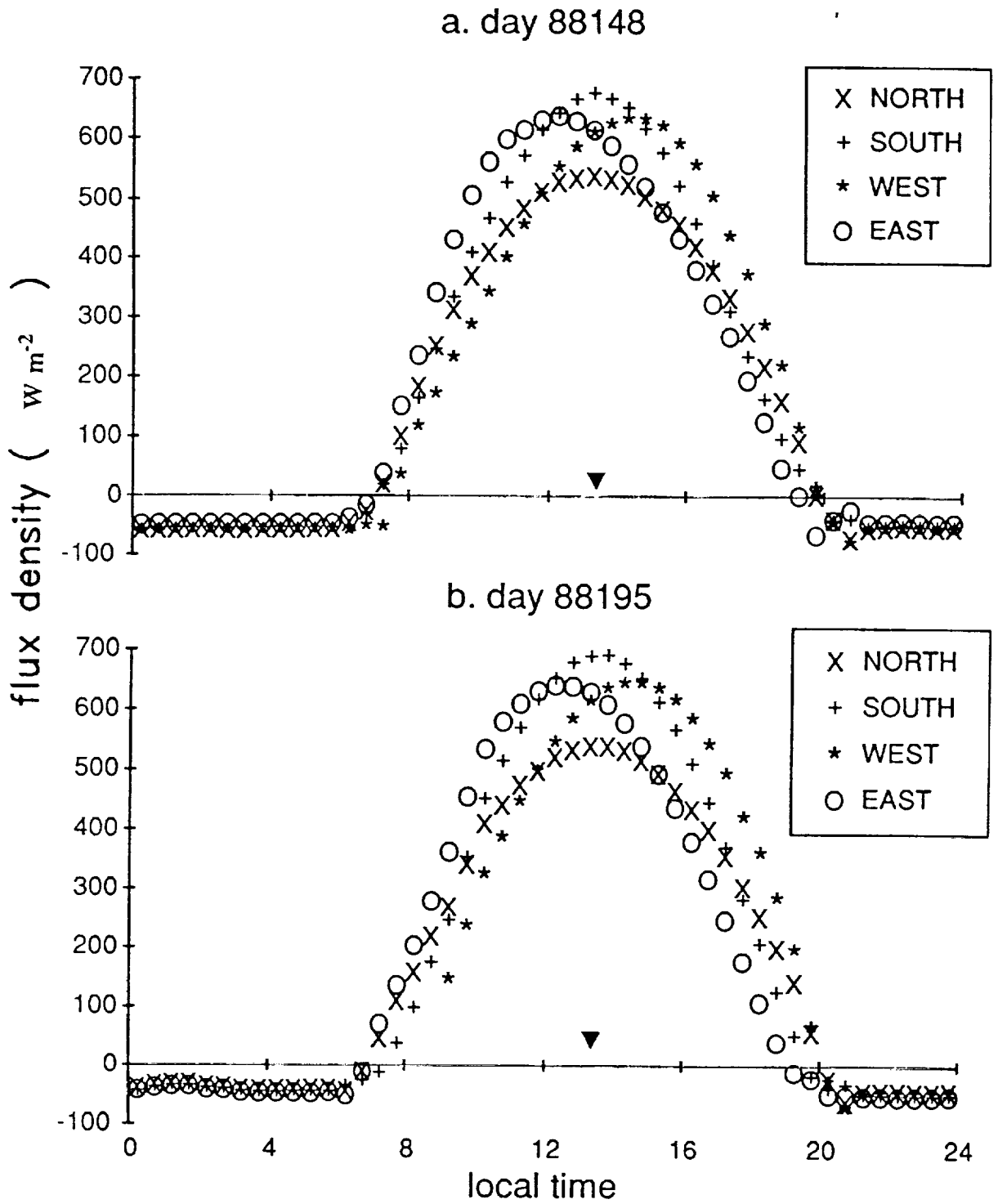


Fig. 2. Diurnal variation of soil heat flux as affected by slope: a. day 148 (May 27, 1988), b. day 195 (July 13, 1988).

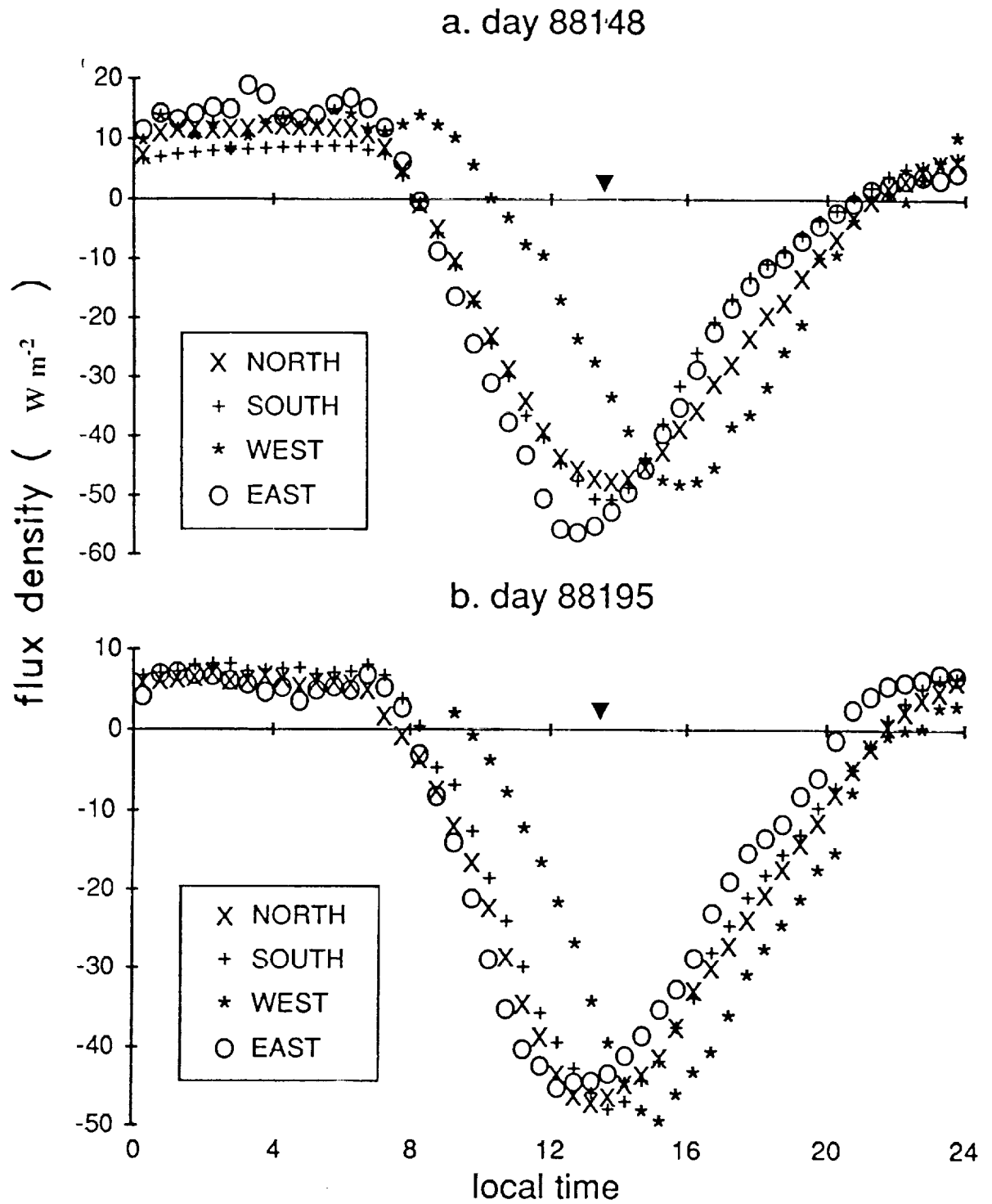


Fig. 3. Diurnal variation of sensible and latent heat fluxes affected by slopes on may 27, 1988: a. sensible, and b. latent.

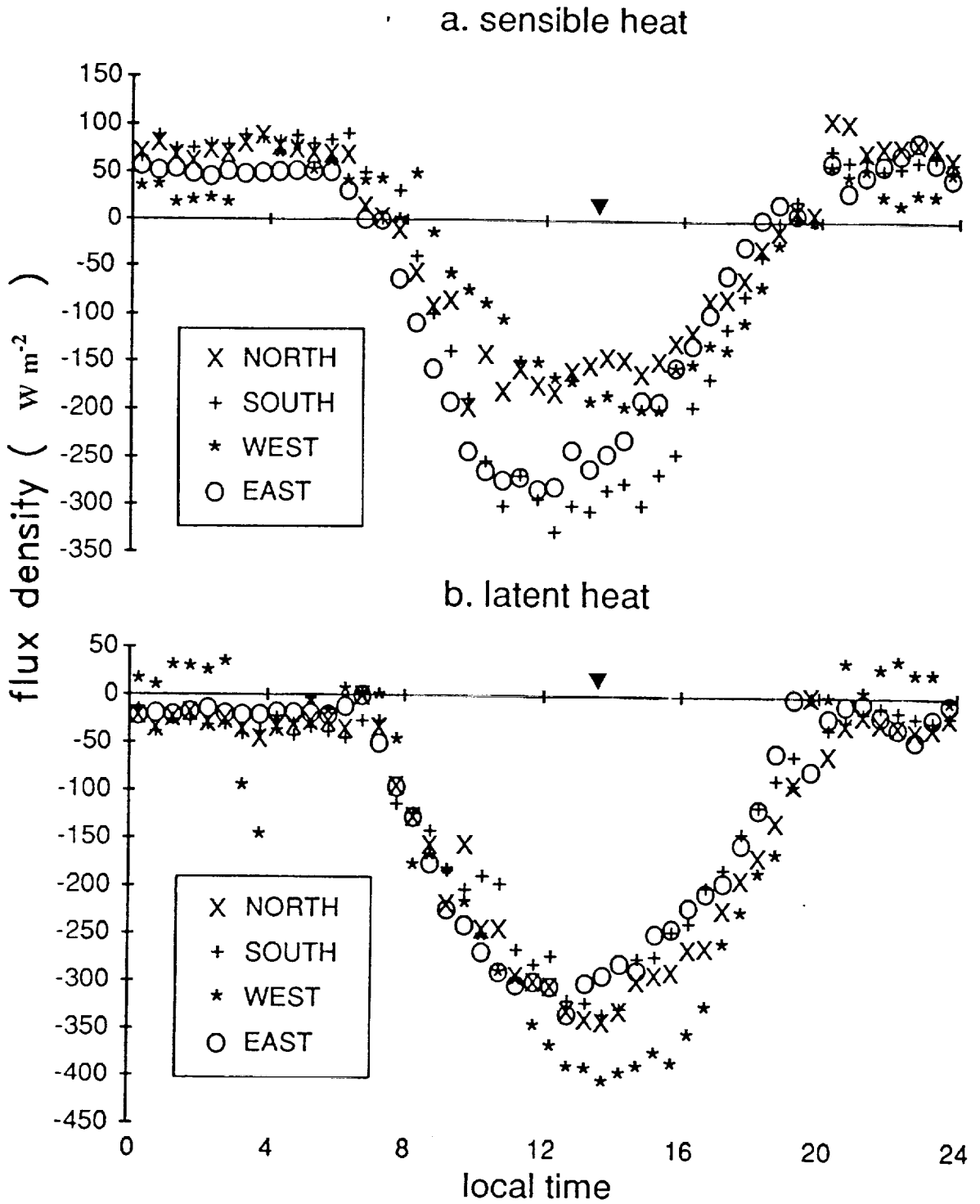


Fig. 4. Diurnal variation of sensible and latent heat fluxes as affected by slopes on July 13, 1988: a. sensible, and b. latent.

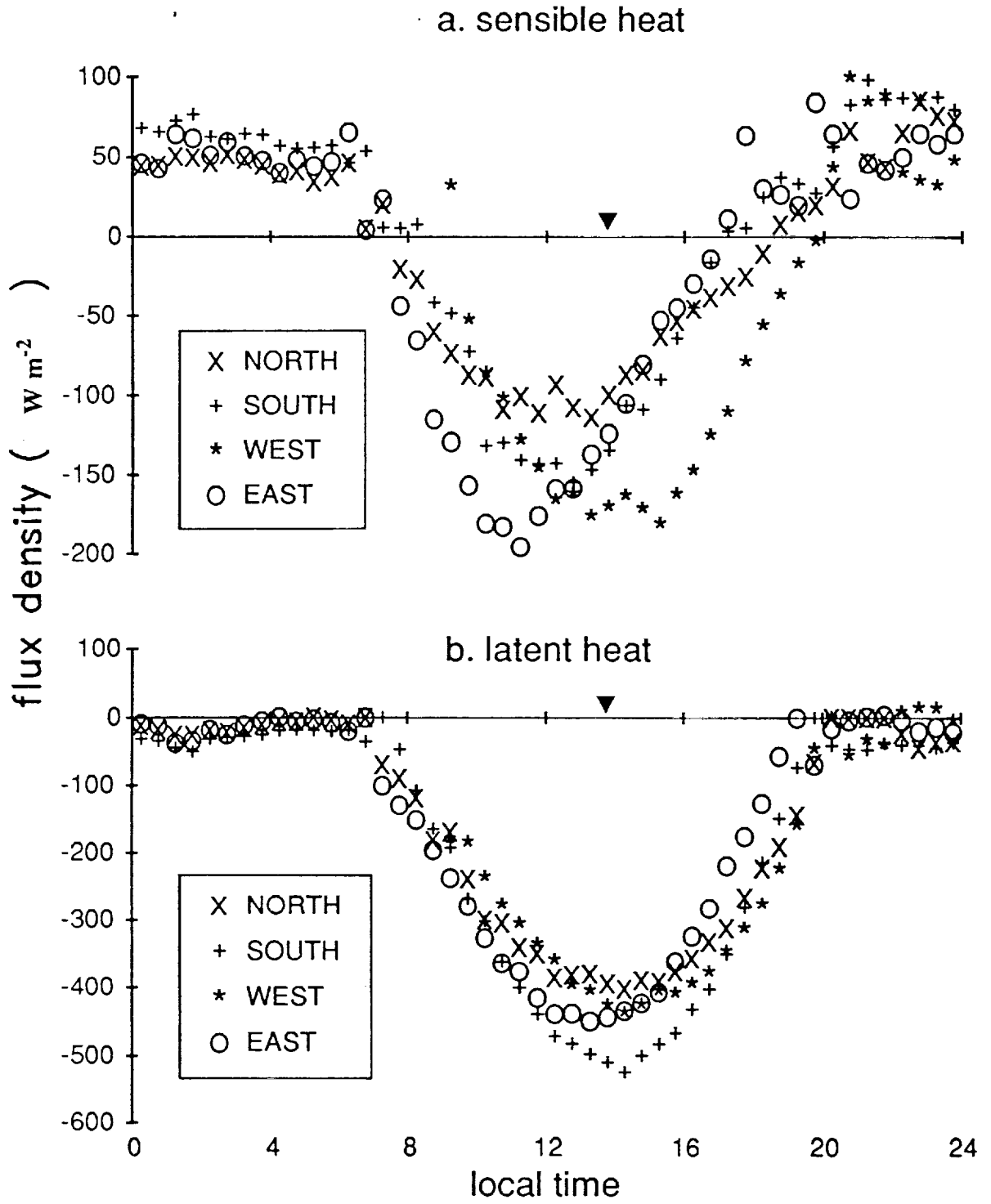
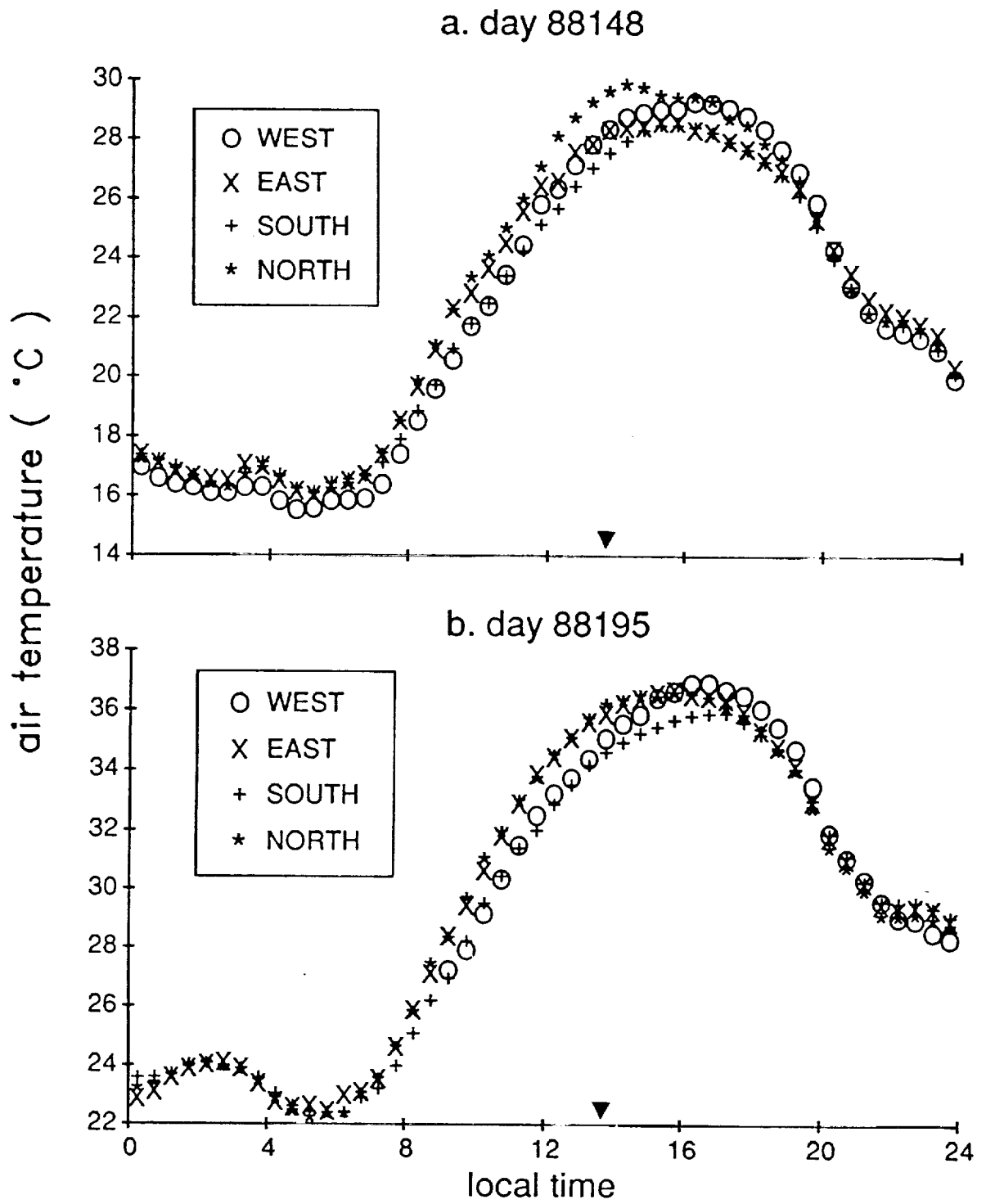


Fig. 5. Diurnal variation of air temperature as affected by slope: a. day 148 (May 27, 1988), and b. day 195 (July 13, 1988).



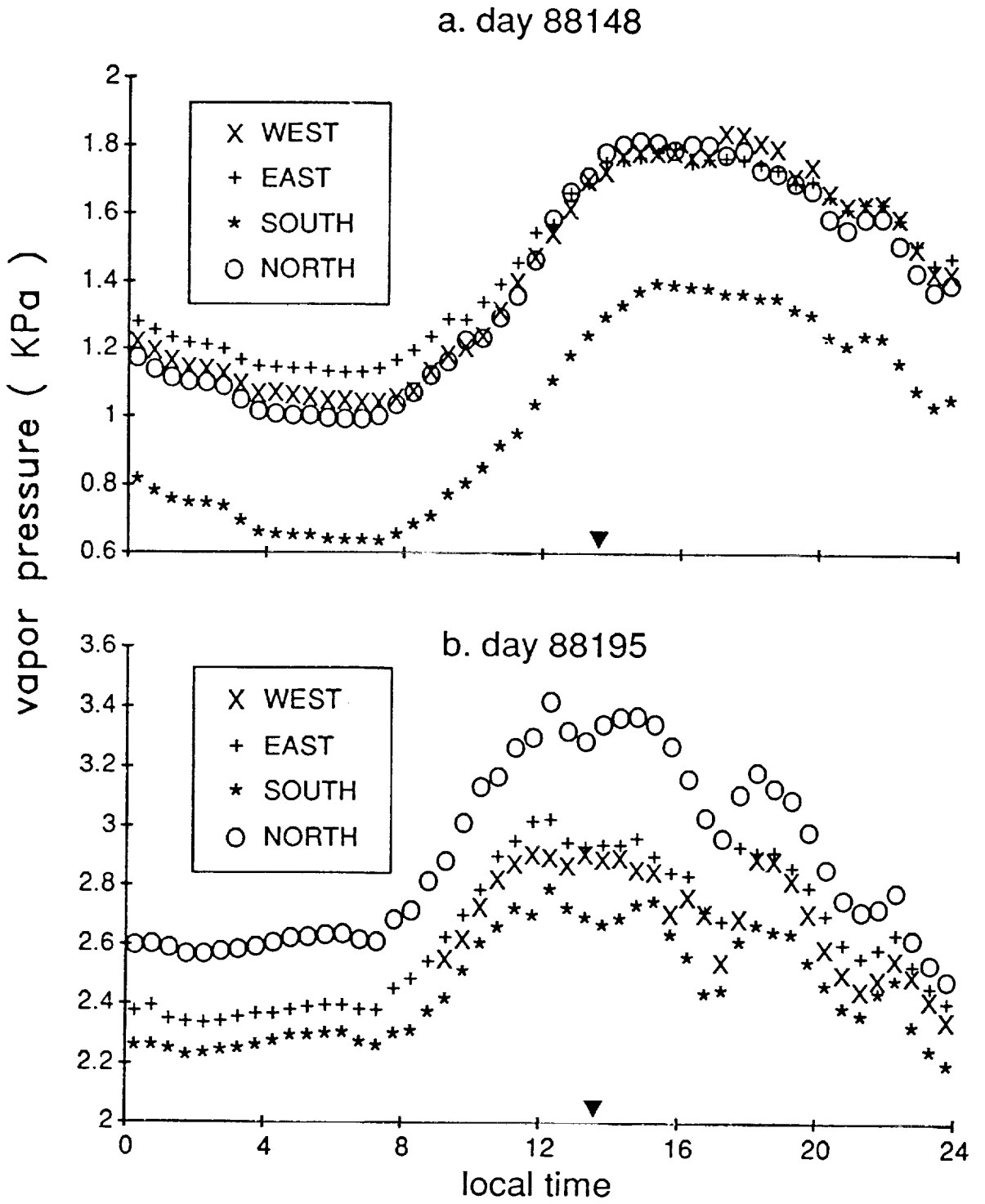
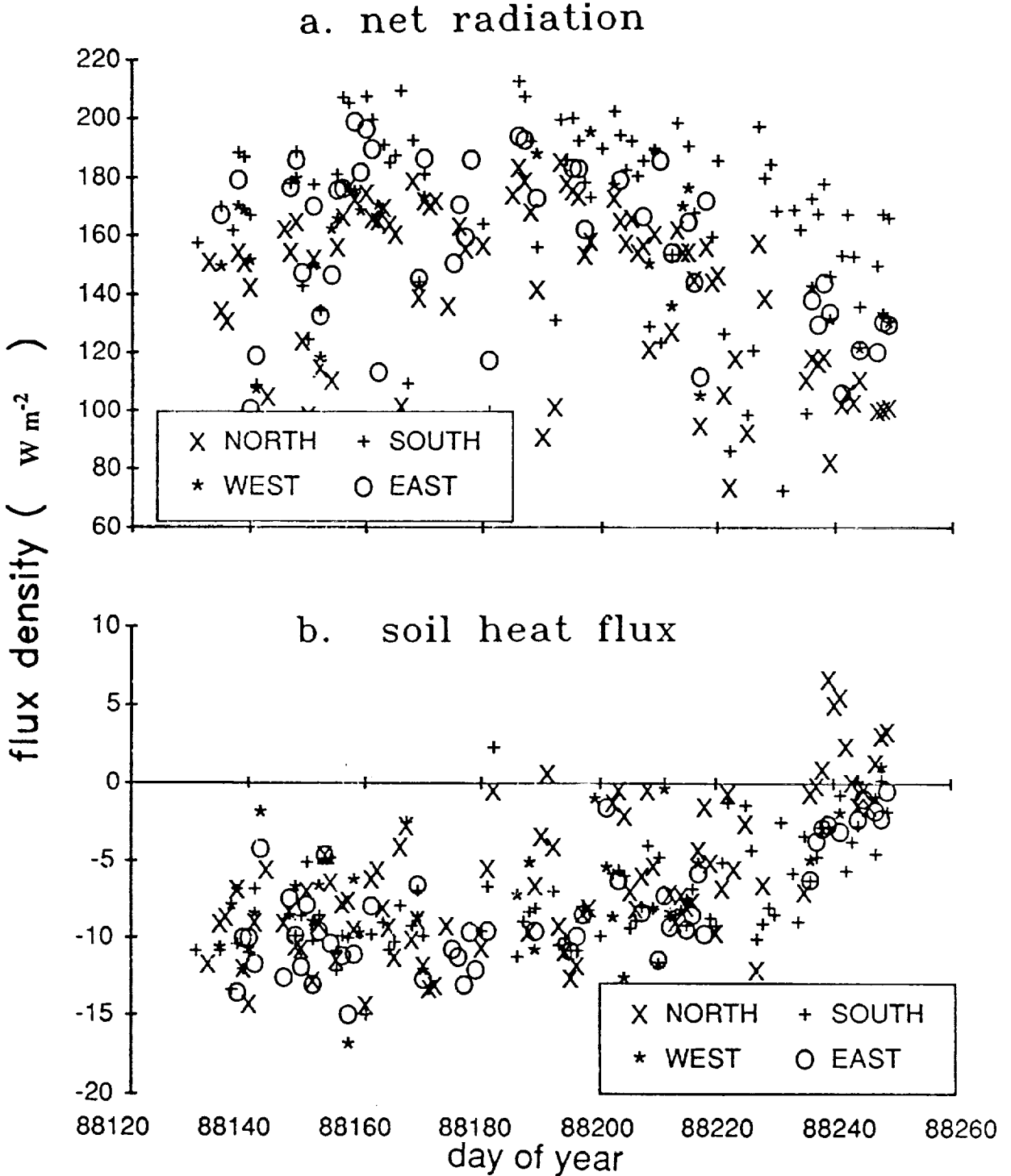
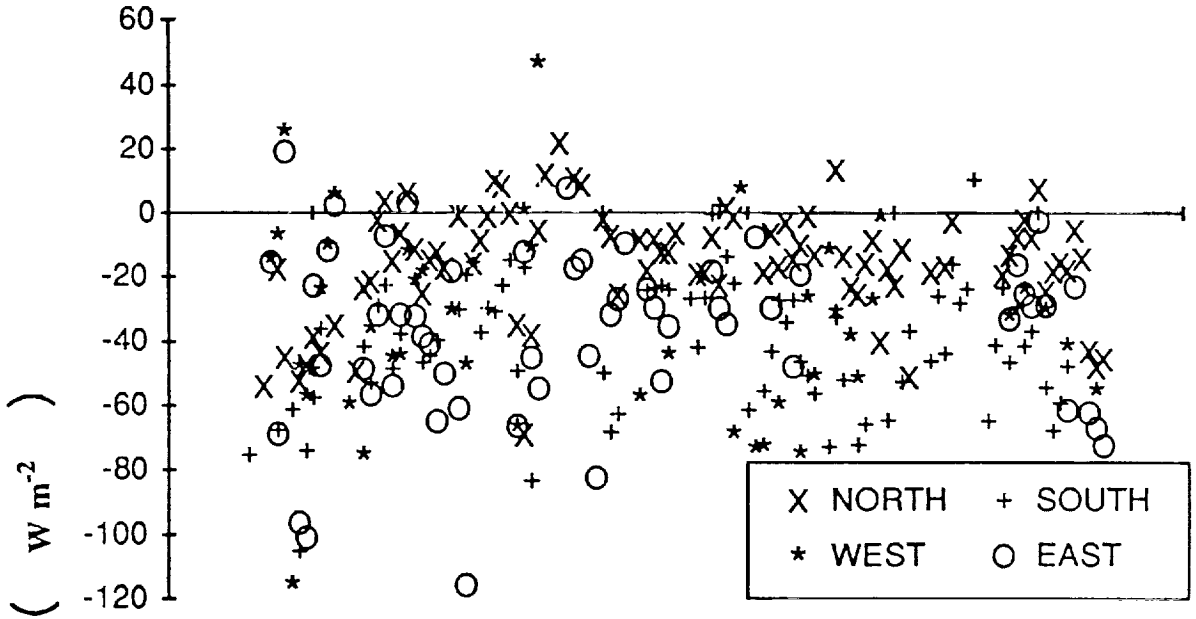


Fig. 6. Diurnal variation of vapor pressure as affected by slope: a. day 148 (May 27, 1988), and b. day 195 (July 13, 1988).

Fig. 7. Seasonal variation of surface energy fluxes as affected by slope: a. net radiation, and b. soil heat flux.



a. sensible heat flux



b. latent heat flux

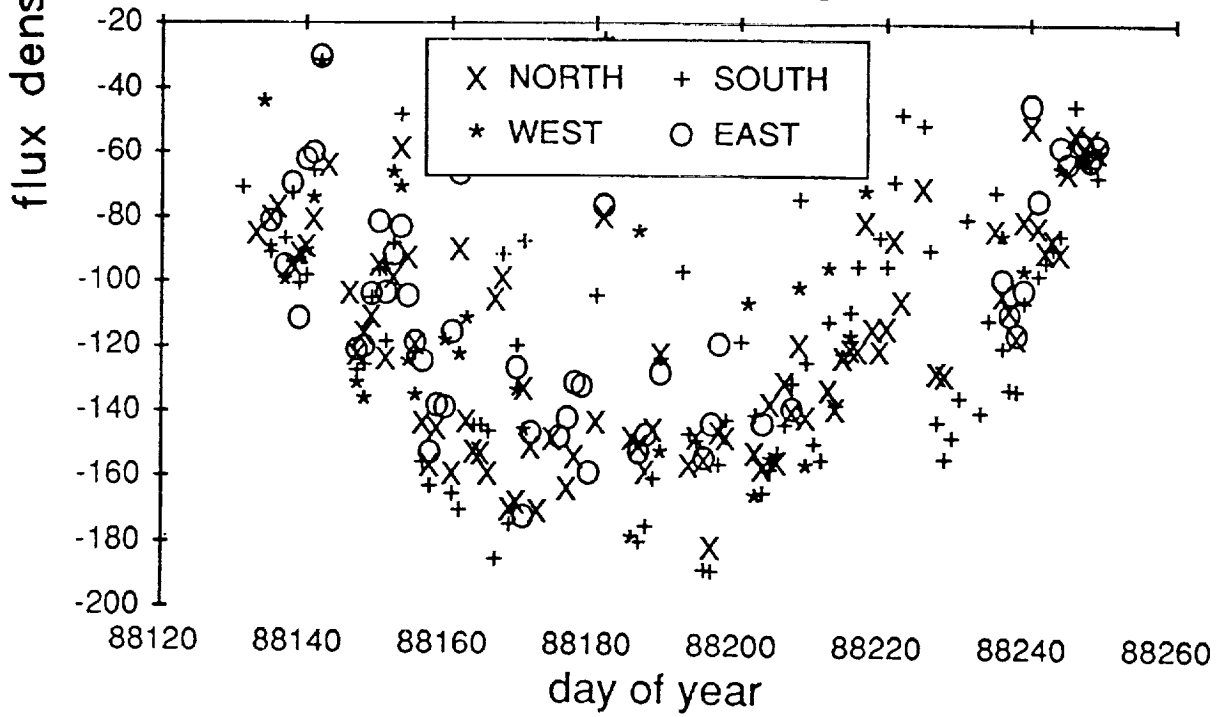


Fig. 8. Seasonal variation of surface energy fluxes as affected by slope: a. sensible flux, and b. latent flux.

Fig. 9. Seasonal variation of soil moisture and leaf area index

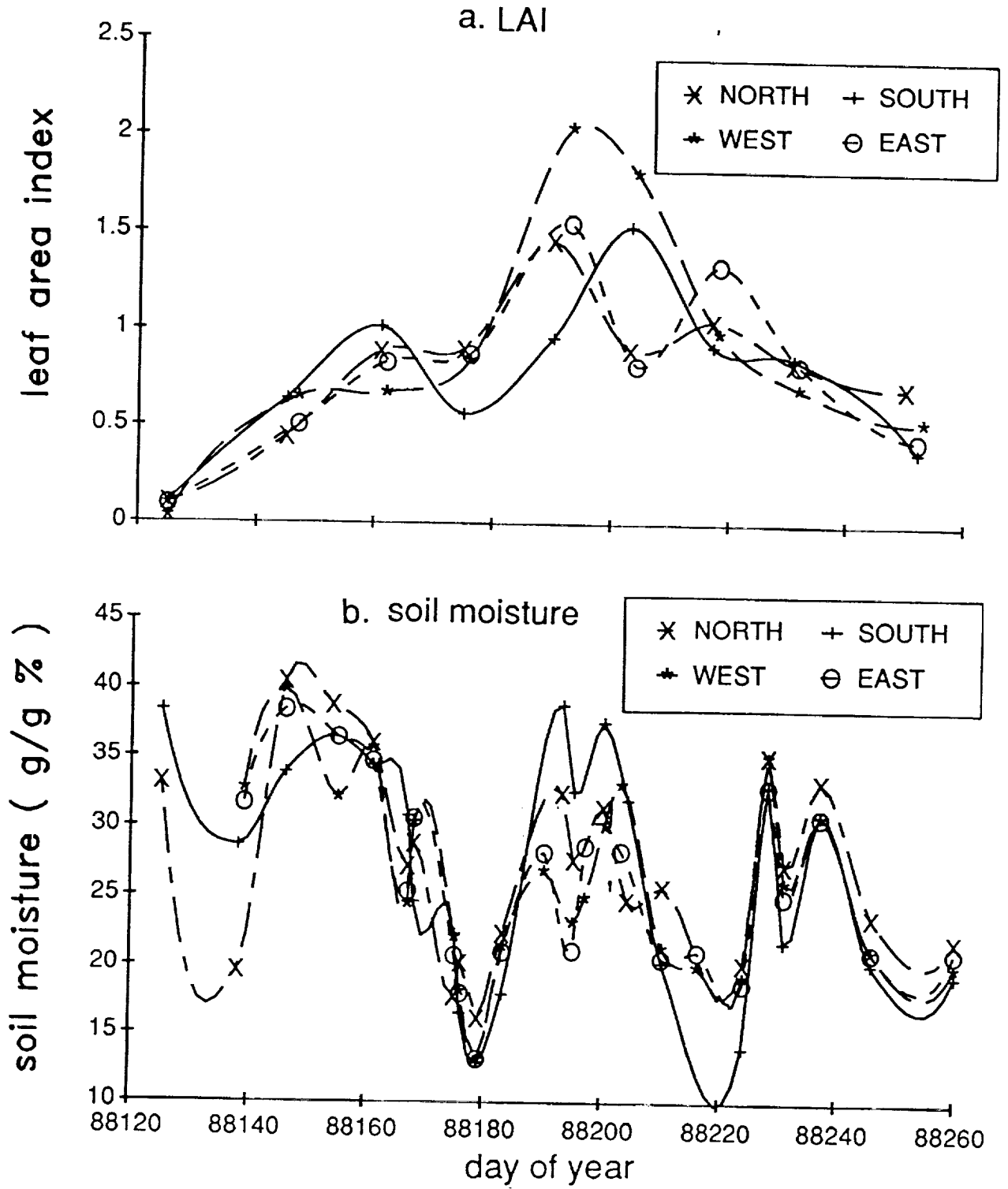


Fig. 10. Seasonal variation of ET as affected by leaf area index on the south-facing slope.

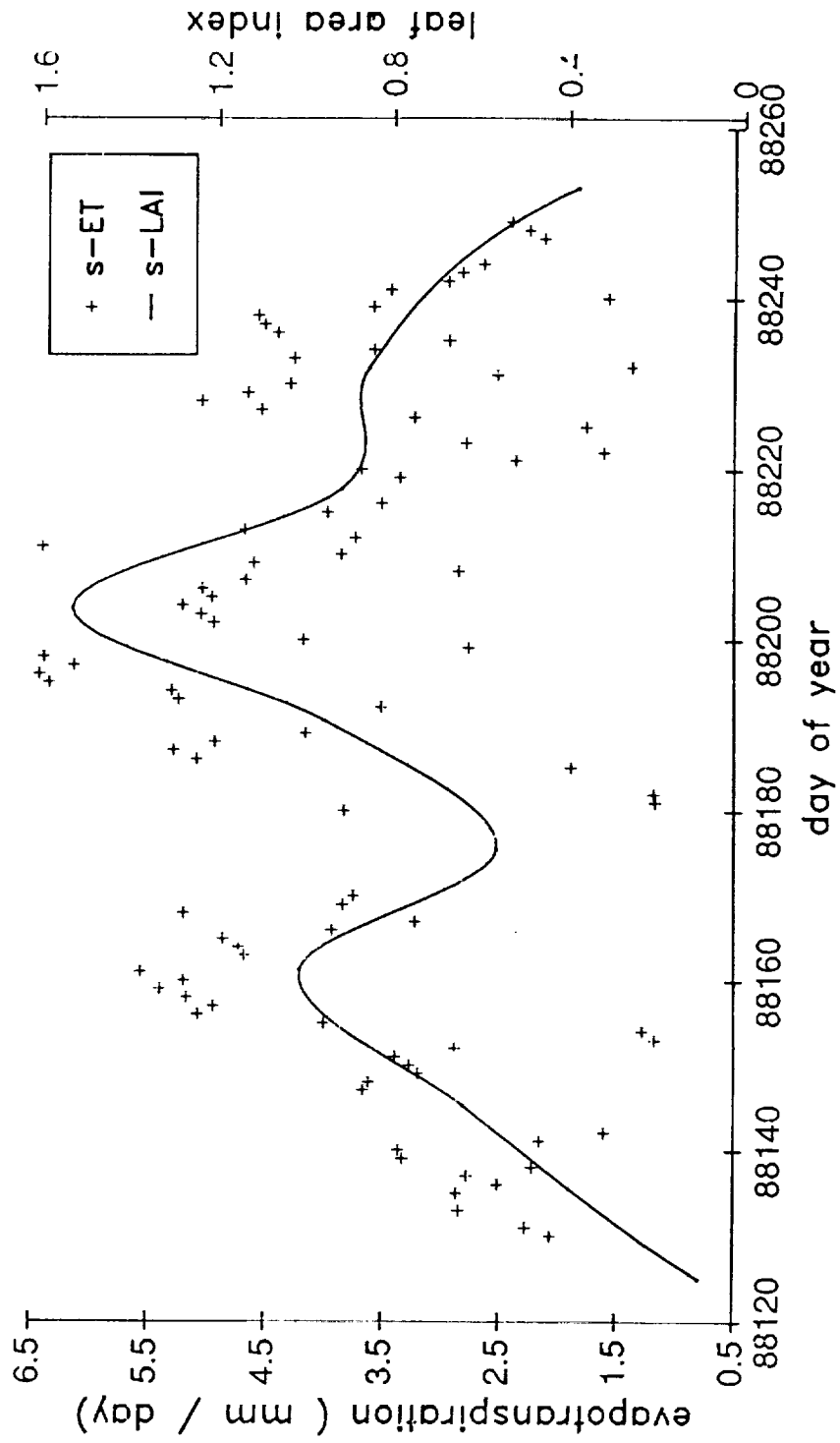


Fig. 11. Seasonal variation of ET as affected by soil moisture on the south-facing slope.

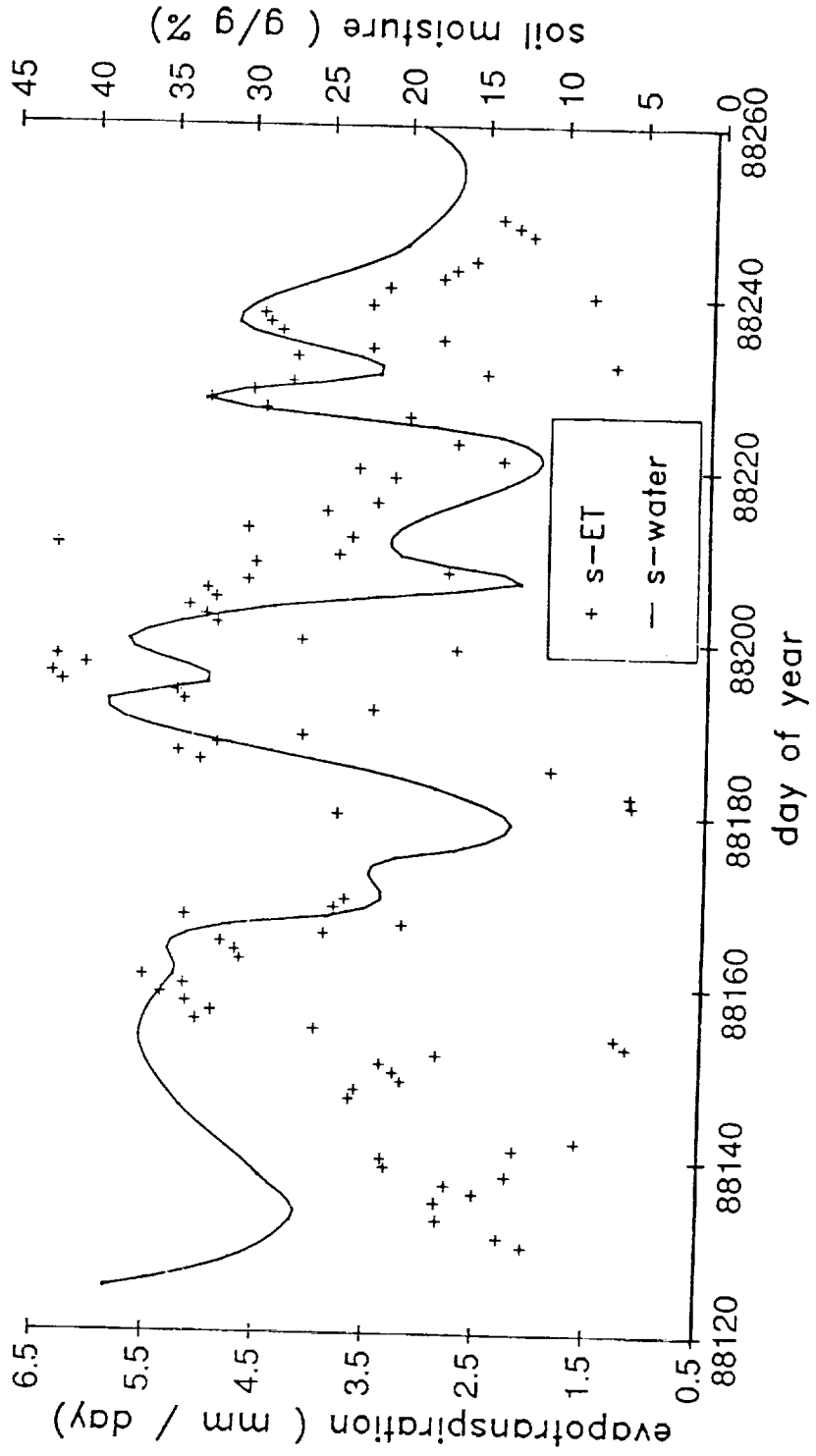


Fig. 12. Seasonal variation of air temperature and vapor pressure as affected by slope: a. air temperature, and b. vapor pressure.

